Archaeological Prospection
Archaeol. Prospect. (2014)
Published online in Wiley Online Library
(wileyonlinelibrary.com) DOI: 10.1002/arp.1496

Structure of an Ancient Egyptian Tomb Inferred from Ground-Penetrating Radar Imaging of Deflected Overburden Horizons

ADAM D. BOOTH[1]*, **KASIA SZPAKOWSKA**[2], **ELENA PISCHIKOVA**[3] AND **KENNETH GRIFFIN**[2]

[1] *Department of Earth Science and Engineering, Imperial College London, South Kensington Campus, London SW7 2AZ, UK*
[2] *College of Arts & Humanities: History and Classics, Swansea University, Singleton Park, Swansea SA2 8PP, UK*
[3] *Director, South Asasif Conservation Project, Supreme Council of Antiquities, Egypt and American University in Cairo*

ABSTRACT Geophysical data acquisitions in most archaeological campaigns aim to image the target structure directly. The presence of a target, however, may be inferred from its interaction with surrounding layers, if its relationship with those layers can be characterized sufficiently. In this paper, we show the use of ground-penetrating radar (GPR) to detect the subsurface continuation of the Ancient Egyptian tomb of the high-official *Karakhamun* (Theban Tomb 223) at the South Asasif tomb complex (Luxor, Egypt). Data were acquired using a Sensors & Software pulseEKKO PRO system, equipped with antennas of 500 MHz centre-frequency, on a silty–sandy sediment surface directly over the target structure. A test vertical radar profile (VRP) suggested that the tomb superstructure was buried too deeply beneath sedimentary overburden to be imaged directly: 500 MHz energy would propagate for only ~2 m before becoming undetectable. Attenuative layers within that overburden were strongly reflective, however, and could be used to provide indirect evidence of any underlying structure. When observed in the GPR grid, these layers showed a discrete zone of deflection, ~0.9 m in amplitude and ~4 m wide, aligned with the long-axis of the tomb. This deflection was attributed either to a collapsed vestibule beneath the survey site, or sediment settling within an unroofed staircase descending from ground- to tomb-floor-level; supporting evidence of this was obtained towards the end of the excavation campaign and in the following year. We highlight the value of such indirect imaging methods as a potential means of improving the capabilities of a given geophysical survey system, in this case allowing the GPR to characterize a target at greater depth than would typically be considered practical. © 2014 The Authors. *Archaeological Prospection* published by John Wiley & Sons Ltd.

Key words: Ground-penetrating radar; Ancient Egypt; South Asasif; tomb; vertical radar profile; stratigraphy

Introduction

Ground-penetrating radar (GPR) methods are well established in archaeological surveying and, despite depth penetration often being limited, provide high-resolution images of archaeological targets (e.g. Conyers, 2013). Provided that the composition of the subsurface is conducive to GPR surveying (e.g. electrically resistive, with freshwater and/or little clay content; Annan, 2005; Weaver, 2006), the shallow range of the GPR system is seldom prohibitive because archaeological features are often located within 1 m of the ground surface. It therefore follows that targets hosted at depth and/or within a more electrically conductive subsurface may be beyond the depth penetration of a GPR wavelet and therefore undetectable by direct GPR means. However, GPR methods may still be valuable in such cases if the buried archaeological target leaves a diagnostic signal within the overburden of its presence at depth: in these circumstances, the archaeological target is not directly imaged but inferred from its effect on the surrounding ground

* Correspondence to: A. Booth, Department of Earth Science and Engineering, Imperial College London, South Kensington Campus, London, SW7 2AZ, UK. E-mail: a.booth@imperial.ac.uk

Received 11 May 2014
Accepted 7 August 2014

conditions. A classic example of such diagnostic signals is the use of cropmarks to delineate archaeological targets (e.g. Featherstone *et al.*, 1999). Equally, from a GPR perspective, the detection of graves (both modern and recent) typically relies not on imaging the human remains but on inferring a burial from the disturbance to overlying soil horizons (Bevan, 1991; Bladon *et al.*, 2012). In order to use indirect evidence to characterize a target, however, it is important to understand the relationship between the target and its host material such that a reliable interpretation can be offered.

In this paper, we describe a series of GPR surveys around an ancient Egyptian tomb complex near the city of Luxor, Egypt (Figure 1). The principle acquisition in this survey was a standard pseudo-three-dimensional (Booth *et al.*, 2008) grid directly over the target area. These data, however, could be reliably interpreted in terms of the target tomb structure only after a series of calibration surveys had been performed, specifically in order to characterize radar propagation through key limestone and sedimentary horizons in the area. These surveys suggested that target structures at the site – a vestibule and staircase at the entrance to the tomb – were probably beyond the depth range of the GPR system, with organic-rich sediment horizons in the overburden providing a barrier to radiowave propagation. The downwards deflection of these horizons, however, provided evidence that an archaeological target was

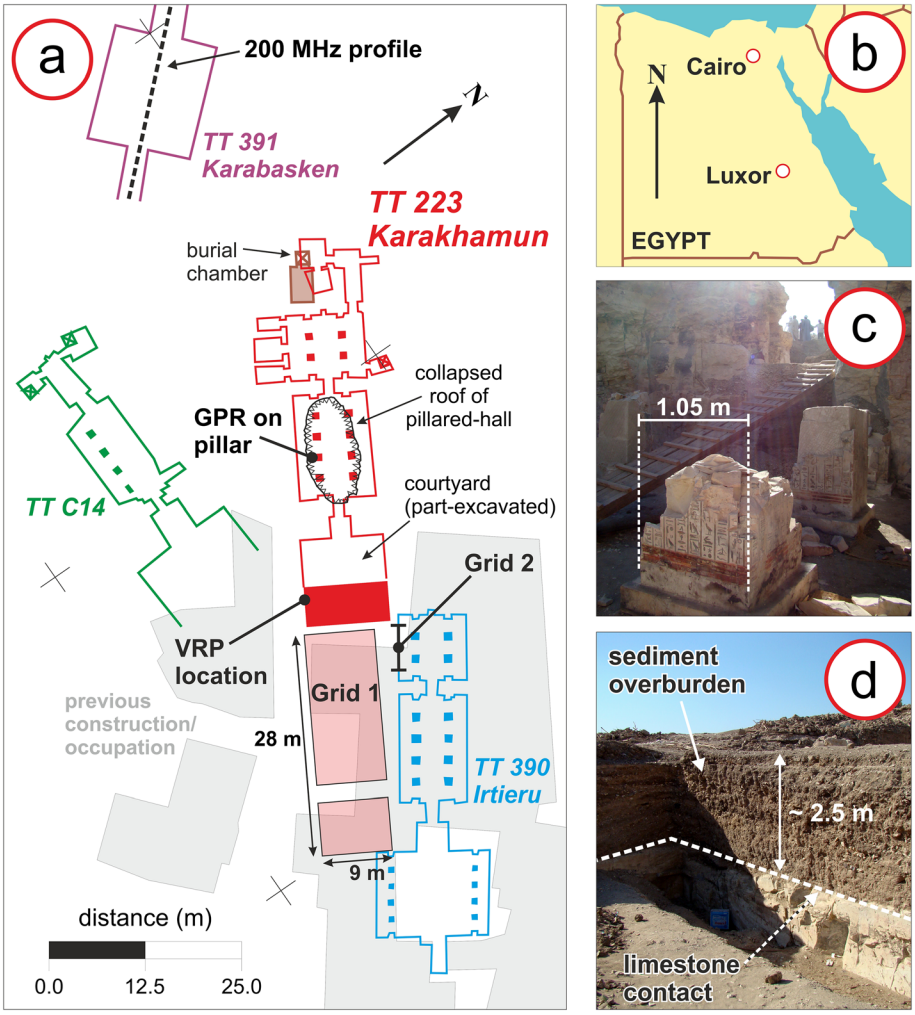

Figure 1. The South Asasif tomb complex, and details of key areas. (a) Tombs at South Asasif, centred on that of *Karakhamun* (TT 223; red) and the GPR investigations around it (labels explained in main text). With the exception of the collapsed pillared-hall of TT 223, all tombs are either completely underground or sediment filled. Digitized from Eigner (1984). b) Regional map: South Asasif is located ~4 km northwest of the Luxor city centre. (c) A view into the courtyard of the *Karakhamun* tomb, undergoing excavation, from inside the pillared hall. The pillar in the foreground was used to calibrate GPR propagation through limestone (Figure 3). (d) A view of excavations in the *Karakhamun* courtyard, in which the contact between the tomb's limestone superstructure and its sedimentary overburden can be seen. The vertical radar profile (VRP; Figure 4) was performed on this sedimentary face. This figure is available in colour online at wileyonlinelibrary.com/journal/arp

DOI: 10.1002/arp

probably present within the subsurface, an inference that was supported on subsequent excavation. We emphasize the potential for geophysical methods to reveal the diagnostic signatures of archaeological remains, even if they themselves cannot be directly imaged.

Archaeological context

The GPR surveys were conducted in support of a programme of archaeological excavations at the South Asasif tomb complex (Luxor, Egypt; 25°43′45″N, 32°36′23″E). The South Asasif tombs (Figure 1) date from the 25th and 26th Dynasties of Ancient Egypt (760–525 BC) (Pischikova, 2014a). Note that this map is digitized from that of Eigner (1984), which itself contains a number of inaccuracies, hence it should be considered a guide to the tomb layout rather than the definitive geometry (a more accurate map is shown later in our final interpretation in Figure 10).

The South Asasif tombs were known, and accessible, in the eighteenth century, and were described as 'beautiful' in the contemporary accounts of travellers (Pischikova, 2014a). They were subsequently lost, however, but rediscovered in 2006 in an extremely dilapidated condition; a village had developed on the site, with domestic structures built over the area (grey areas in Figure 1a) and farm animals were kept in and around the tombs. Conservation efforts have therefore been ongoing since 2006 (Pischikova, 2014a). The largest and highest-status tomb in the complex is that of the high-official *Karakhamun*, denoted as 'TT 223' (TT being an abbreviation for 'Theban Tomb'). Unfortunately, TT 223 is in a particularly poor condition. Originally, its two 'pillared halls' were subterranean (excavated directly into the local limestone bedrock) but these have collapsed and are now unroofed (e.g. Figure 1c); by contrast, its originally open-air courtyard is now sediment-filled and is the focus of concentrated excavation (Figure 1d). However, where TT 223 is intact, its decoration is testimony to the high status of *Karakhamun*; his sunken burial chamber features a so-called 'celestial scene' similar to larger examples in the pharaonic tombs of the Valley of the Kings. Neighbouring TT 223 within the South Asasif complex are the tombs of an unknown individual, previously misidentified as *Ankhefendjehuti* (TT C14), and *Irtieru* (TT 390), and that of *Karabasken* (TT 391) is further west (Eigner, 1984) (Figure 1a). Although these other tombs are smaller and less ornate than TT 223, they are currently in a better state of preservation (Pischikova, 2008, 2009, 2014b).

Tomb TT 223 is similar in style and age to the well-preserved tomb of *Pabasa* (TT 279), located close to the Temple of Hatshepsut. Tomb TT 279 features pillared halls and an open courtyard (Figure 2a), but also a vestibule at the entrance to the tomb, and a stone staircase that descends from the ground surface to the floor-level of the tomb. It was expected that the tomb of *Karakhamun* would feature equivalent structures (Figure 2b), but these had not been confirmed at the

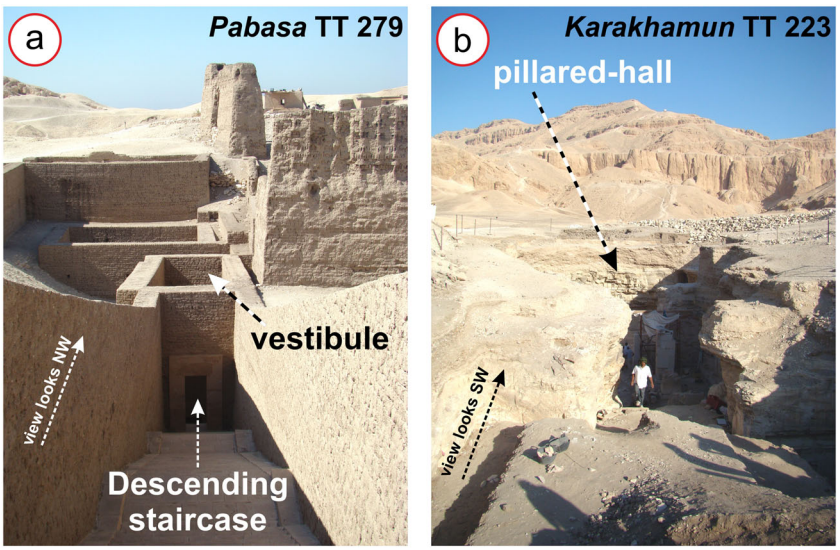

Figure 2. Analogous tombs from the Luxor area: (a) The tomb of *Pabasa* (TT 279), (b) the tomb of *Karakhamun* (TT 223). Both tombs are viewed from the same relative viewing angle, specifically from the exterior, looking along their long axis into the inner chambers. The tomb of *Pabasa* shows the original construction condition of that of *Karakhamun*, and features a descending staircase and vestibule in front of internal courtyards and pillared halls. The presence of the staircase and vestibule of TT 223 are the targets of the GPR survey described here. This figure is available in colour online at wileyonlinelibrary.com/journal/arp

DOI: 10.1002/arp

time of the 2011 excavations and survey. The aim of the GPR survey was therefore to provide evidence of any such structures immediately outside (east) of the tomb's courtyard, to allow further excavations to be scheduled in the following years.

Tomb construction and GPR detection potential

The superstructure of each of the South Asasif tombs is cut into natural limestone. Tomb TT 223 is overlain by ~2.5 m of sandy/silty desert sediment (see contact in Figure 1d) and its limestone roof is around 1 m thick (Pischikova, 2014a). Any underlying chambers are also expected to be sediment-filled, as a result of flash-flooding, but with a remnant air-gap beneath the ceiling. It is this air-gap that would ordinarily be the target of a GPR survey. Although this is ostensibly a good GPR target, the total depth of the target is approximately 3.5 m, and this could be problematic for the GPR systems that are conventionally deployed for an archaeological survey. In order to explore the GPR propagation potential through the various materials around the tomb complex, a series of preliminary surveys were performed. These tests, and all subsequent surveys, were performed with a Sensors & Software pulseEKKO PRO GPR, equipped with antennas of 500 MHz centre frequency, unless otherwise mentioned.

To characterize the GPR propagation through limestone, 500 MHz antennas were placed directly on the planar surface of a ruined column base in the pillared hall (Figure 1c). These columns are square in plan view (and hence represent flat surfaces for transmission and reflection) with a width of 1.05 m; these pillars represent original bedrock because the tomb was excavated around them, hence characteristics measured here should be representative of the wider superstructure. There is no evidence of inhomogeneities within the pillar (e.g. fractures or veins) on any of its faces and it is therefore assumed that the limestone is homogeneous. The recorded GPR trace (Figure 3) shows direct GPR arrivals, and a primary reflection and its first multiple from the opposite face of the column; a second multiple is not detectable above background noise. No other events are detected within this trace, suggesting that the limestone within the pillar is indeed homogeneous. The strong first multiple implies that 500 MHz GPR energy is able to propagate and remain detectable for at least 4.2 m through the local limestone (i.e. four travel-paths between the faces of the pillar), but will be critically attenuated after 6 m. Furthermore, as expected, there should be a strong reflection from the

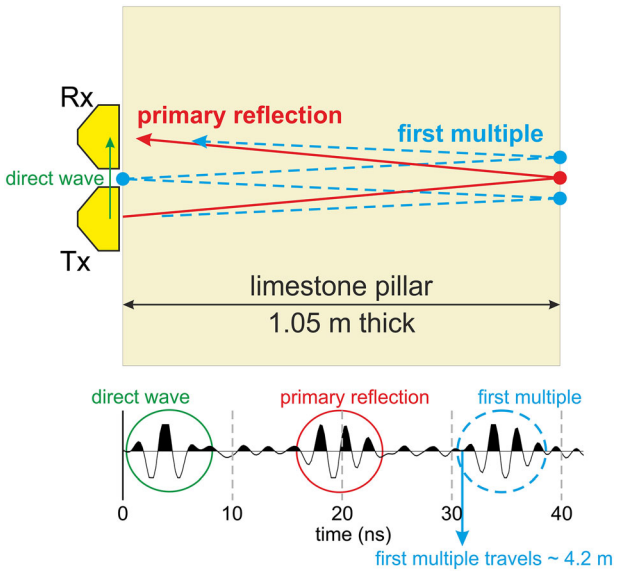

Figure 3. Test of GPR propagation through limestone. The 500-MHz antennas are placed on the planar face of a pillar, 1.05 m wide (shown schematically), and the recorded trace is the summation of 40 individual acquisitions (scaled with automatic gain control, 10 ns window). The trace shows a clear reflection (red) from the opposite face of the pillar, and also a multiple (blue). These arrivals suggest that 500 MHz energy is able to propagate over 4 m through limestone before being undetectable. This figure is available in colour online at wileyonlinelibrary.com/journal/arp

interface between the ceiling of any buried chamber and the underlying air-gap. The efficiency of GPR propagation through limestone is consistent with observations made by other authors (e.g. Creasman and Sassen, 2011; Welc *et al.*, 2013) and the implied GPR velocity of 0.135 m ns^{-1} (derived from the 15.6 ns arrival time of the first reflection) is similar to reported limestone velocity values (e.g. Annan, 2005).

To investigate propagation through the sediment overburden of the tomb, a VRP (vertical radar profile; e.g. Buursink *et al.*, 2002; Vignoli *et al.*, 2012) was performed on the exposed vertical wall of the courtyard excavation. The overburden consists of loose and dry sandy–silty material, but features some prominent 'organic-rich' layers, presumably originating from the farm animals kept around the site; one such layer is present within the depth range sampled in the VRP, representing the only significant inhomogeneity within the vertical section. For the VRP acquisition, the 500 MHz transmitter (*Tx*) was held stationary while the vertical offset to the receiver (*Rx*) was increased in increments of 0.05 m. The VRP data (Figure 4) show prominent direct air- and ground-wave arrivals, with the latter expressing a velocity of 0.171 ± 0.003 m ns^{-1} (established from a best-fit straight line to travel times). Such a high velocity is consistent with the very loose nature of the overburden, and a

DOI: 10.1002/arp

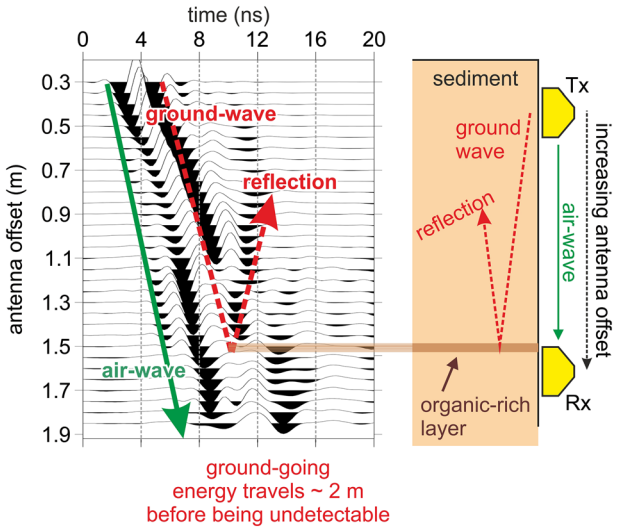

Figure 4. Test of GPR propagation through sedimentary overburden. The 500 MHz antennae are used to acquire a vertical radar profile (VRP) (shown schematically). Ground-going energy is undetectable after travelling for ~2 m; furthermore, there is no evidence of energy transmitted through an 'organic-rich' layer at position 1.45 m, suggesting that the layer is attenuative but strongly reflective to radar energy. This figure is available in colour online at wileyonlinelibrary.com/journal/arp

high proportion of air-filled porosity. There is also a prominent reflection from the organic-rich layer at an offset of 1.45 m; however, the layer appears to block the transmission of energy to greater depths as no direct arrival is seen beneath it. It therefore appears that the organic-rich layers could be barriers to GPR propagation, and therefore problematic for imaging the buried superstructure of the tomb.

Prior to commencing the main survey (see below), a 200 MHz common-offset (CO) profile was performed over the known superstructure of the tomb of *Karabasken* (TT 391; Figure 1a) to investigate depth penetration with this lower-frequency system; no reflections from the tomb could be detected. Although TT 391 is located beneath a thicker sediment cover, the potential to image directly the superstructure of TT 223, with either 500 or 200 MHz antennas, was therefore deemed to be low.

The GPR surveys to detect the TT 223 superstructure

Following these initial tests, two grids were nonetheless established to detect evidence of the *Karakhamun* tomb beyond the present extent of excavation. Grid 1 (see below) was located on a flat surface immediately east of the courtyard: in addition to likely problems of depth penetration, acquisitions were located over modern building foundations, which could complicate interpretation. Given these concerns, grid 2 (see below) was a series of vertical acquisitions (Jol *et al.*, 2006) performed on the limestone wall of the *Irtieru* tomb, with the aim of detecting any continuation of the *Karakhamun* tomb from this subsurface location. Both these acquisitions were pseudo-three-dimensional CO grids (Booth *et al.*, 2008) using shielded 500 MHz antennae, having cross-line sampling intervals of 0.25 m, respectively. This cross-line density does not fulfil full-resolution sampling criteria (Grasmueck *et al.*, 2005) for either grid although it may be sufficiently dense to facilitate trace interpolation (Booth *et al.*, 2008; Li, 2012); however, time-slices could be interpreted without this additional processing step. Trace recording was triggered with a calibrated odometer wheel (pressure was maintained against the axle of the wheel to ensure continuous contact with the vertical wall in the case of the second grid).

Grid 1: surface survey outside the TT 223 excavation

Grid 1 profiles were orientated parallel to the short axis of the grid (perpendicular to the long axis of the tomb; Figure 1a), with each CO profile starting at its southern edge and having a spatial sampling interval of 0.05 m. The grid extended for 28 m from the edge of the courtyard excavation, although contained a gap in coverage due to the presence of recent concrete debris visible at the ground surface. Data were processed in Sandmeier ReflexW© software, using dewow (5 ns time window) and bandpass (corner frequencies of 120–200–500–1100 MHz) filters, time-zero static corrections and Kirchhoff migration (with a migration aperture of 1 m (21 traces) and a constant velocity of 0.11 m ns^{-1}). This velocity is rather lower than the value observed in the VRP analysis, and is representative of the velocity expressed by the best-fit curve to a number of diffraction hyperbolae. The reduction in velocity at this location is attributed to a greater degree of compaction in the overburden layers: not only was the VRP recorded on a free sediment face, which had been exposed for several months and was crumbling during the acquisition, areas of grid 1 were occupied by buildings (see Figure 1), hence the subsurface could have undergone more compaction. The use of constant velocity migration is clearly a source of error in interpreting the geometry of reflections, but no additional velocity information could be derived to define a more sophisticated model (indeed, reflection hyperbolae in a common midpoint (CMP) gather acquired

DOI: 10.1002/arp

within grid 1 did not express sufficient travel-time move-out to provide a reliable velocity estimate).

Two profiles from this grid are shown in Figure 5, with their positions in the grid shown in Figure 6. In Figure 5b, there is a prominent 'V-shaped' reflection, which is absent in Figure 5a and any other profile acquired within 5 m from the edge of the *Karakhamun* excavation. The 'V' becomes progressively more pronounced, and deeper, with increasing distance from the tomb, with its vertex reaching a maximum of ~20 ns travel-time (~1.1 m depth, assuming a constant velocity of 0.11 m ns^{-1}) beneath the ground surface. Beyond ~15 m from the excavation, the 'V' is again not present.

The flanks of the 'V' can also be observed in a cross-line extracted from the grid (Figure 5c), and in time-slices (Figure 6a). Despite the undersampled nature of the GPR wavefield in the cross-line direction (and the lack of migration therefore applied in this direction), the onset and maximum depth extent (~1.15 m) of the 'V' can be perceived, with the flank between 6 and 9 m through the profile appearing steeper than that between 10 and 16 m. In time-slices, the southern flank of the 'V' becomes prominently evident as travel-time exceeds 6 ns, and its northern flank appears beyond 9 ns. These flanks gradually migrate across the survey grid (dashed lines in Figure 6b) until they coalesce into a closed hollow. The maximum depth of this hollow, however, is shallower than the anticipated depth of the tomb superstructure beneath the sediment overburden. Note that in the shallowest slices of Figure 6a, the footprint of former occupation is present but

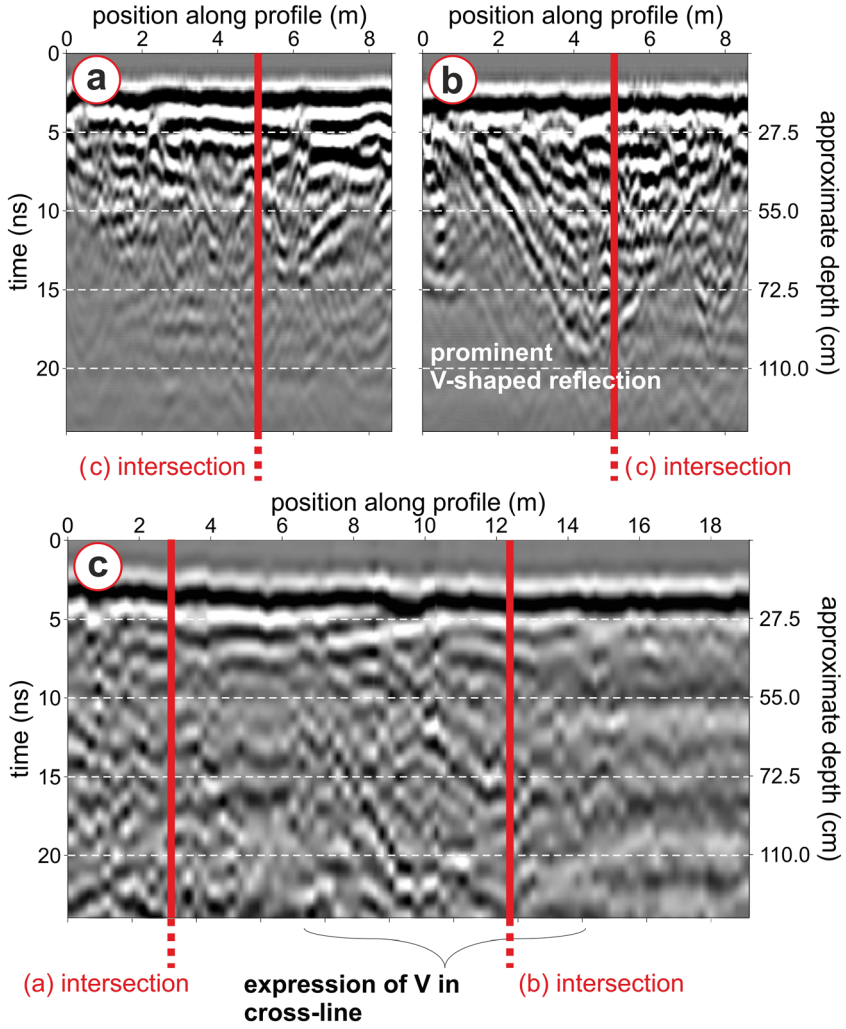

Figure 5. Example GPR CO profiles through grid 1, located at the surface immediately east of the *Karakhamun* courtyard excavation. (a) Profile 2.75 m from the western edge of the grid (see Figure 6). (b) Profile 12.25 m from the western edge of the grid (see Figure 6). The profile in (b) features a prominent 'V-shaped' reflection, which is absent in (a). (c) Cross-line through the GPR grid, at a distance of 5.25 m along profiles (a) and (b) (intersections marked as red lines). The 'V-shaped' reflection is also observed in this profile. This figure is available in colour online at wileyonlinelibrary.com/journal/arp

DOI: 10.1002/arp

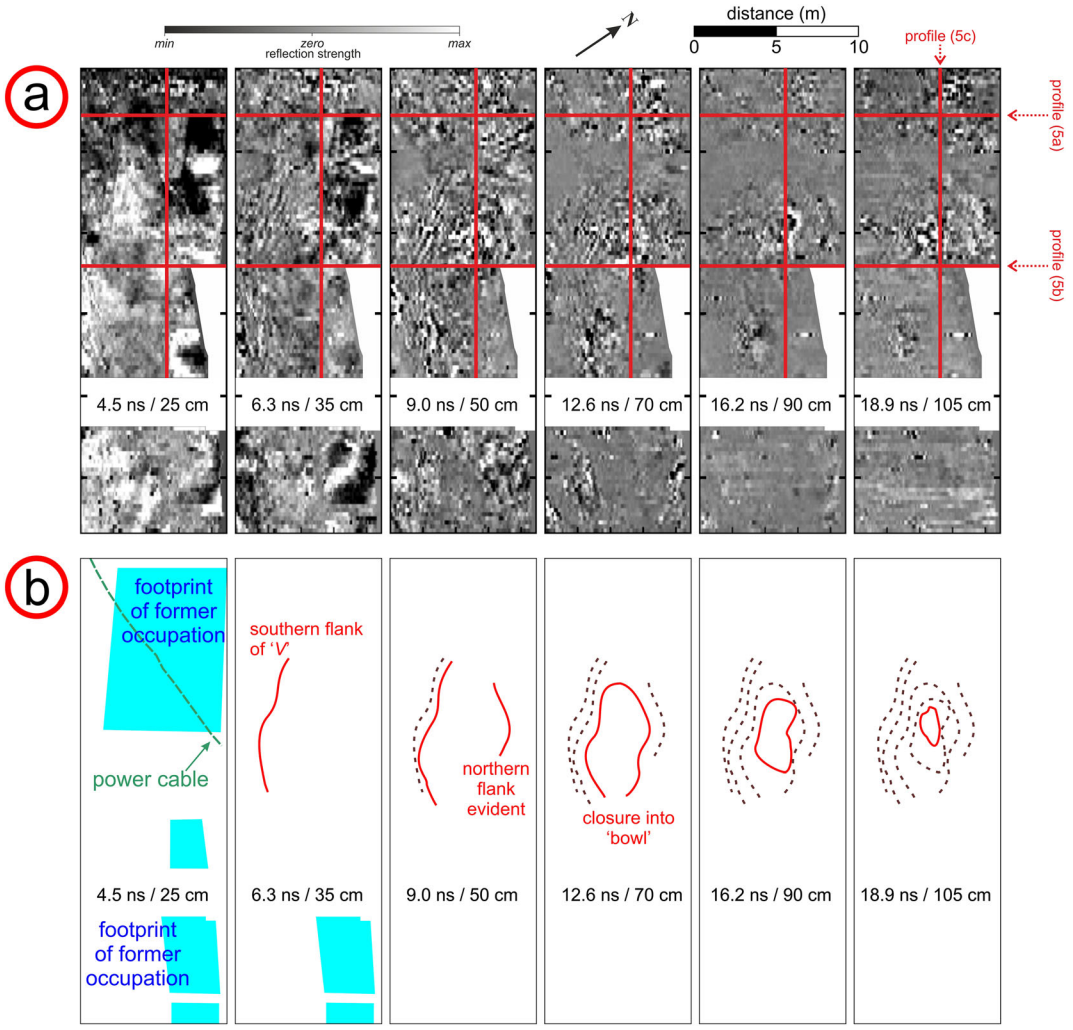

Figure 6. Time-slices and interpretation of data in grid 1, becoming progressively deeper from left to right. (a) Uninterpreted data. No amplitude processing is applied in the generation of these slices beyond the algorithms listed in the main text. Red lines show positions of profiles in Figure 5. Depths are calculated using a constant velocity of 0.11 m ns^{-1}. (b) Interpreted slices. The shallowest slices evidence the footprint of modern occupation at the site; thereafter the flanks of the 'V-shaped' feature can be seen migrating through the grid (solid red lines; the dashed lines mark the position of the flanks in previous slices). This figure is available in colour online at wileyonlinelibrary.com/journal/arp

evidence of this beyond ~ 35 cm depth does not persist. The linear feature observed in the shallowest slice (green in Figure 6b) is an electricity cable passing through the survey grid into the *Irteriu* tomb.

Grid 2: vertical grid on the internal wall of TT 390

The GPR survey on the pillar (Figure 3) suggested that 500 MHz energy could be detectable even after propagating 4 m through limestone. The map of the South Asasif tombs (Figure 1) implied that any eastward continuation of the *Karakhamun* tomb could pass close to that of *Irtieru*; if the walls of the two tombs are within 2 m of each other, it is possible that TT 223 could be detected from within TT 390. The internal wall of TT 390 is planar and therefore suitable for GPR surveying. A horizontal line was defined on the tomb wall to mark the start of each CO profile, approximately 2.1 m above the floor level such that the first survey position was reachable at 'full stretch' by an operator but without requiring ladders or additional support. Grid 2 was therefore 2 m high, and covered a 6.3 m span of the *Irteriu* internal wall, with each vertically orientated profile having a spatial sampling interval of 0.02 m.

No coherent reflections were detected within the *Irtieru* grid that could be associated with the continuation of the *Karakhamun* tomb. The *Karakhamun* tomb may be sediment-filled at this location, hence it is possible that reflectivity may be lower than implied in the analysis in Figure 3, since a limestone–sediment

DOI: 10.1002/arp

interface represents a weaker electromagnetic contrast than limestone–air interface, particularly if that sediment is dry (e.g. Witten *et al.*, 2000). Certain profiles (e.g. Figure 7) show some reflectivity, apparently trending parallel to the surface of the wall, but this is rarely continuous across several profiles and is therefore attributed to local heterogeneities in the limestone rather than a continuation of the *Karakhamun* superstructure. As no strong and/or continuous reflectivity is perceived within grid 2, we therefore suggest that any continuation of the *Karakhamun* tomb does not pass within 2 m of the rear chamber of TT 390. The propagation range of GPR energy could have been increased using the 200 MHz antennas, but these are unshielded hence data may have been strongly contaminated with coherent airwave noise and target reflections may have in any case been obscured (note: no such problems were evident in the 500 MHz record).

Summary of results

Figure 8 shows a summary of results and inferences from the two survey grids. The 'V-shaped' reflection from grid 1 is picked and depth-contoured (assuming a velocity of 0.11 m ns^{-1}), and forms a bowl-shaped anomaly aligned almost parallel with the long axis of the tomb in the preliminary Eigner (1984) map. As stated above, the bowl reaches a maximum depth of 1.1 m from the ground surface (a maximum vertical deflection of ~0.9 m) and is ~4 m wide.

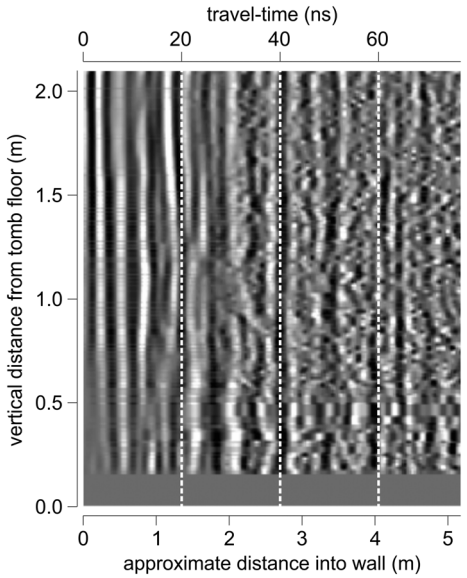

Figure 7. A GPR profile extracted from grid 2, acquired as a vertical CO profile on the internal wall of the *Irtieru* tomb. No coherent reflections can be identified within this grid that could correspond to the subsurface continuation of the *Karakhamun* tomb.

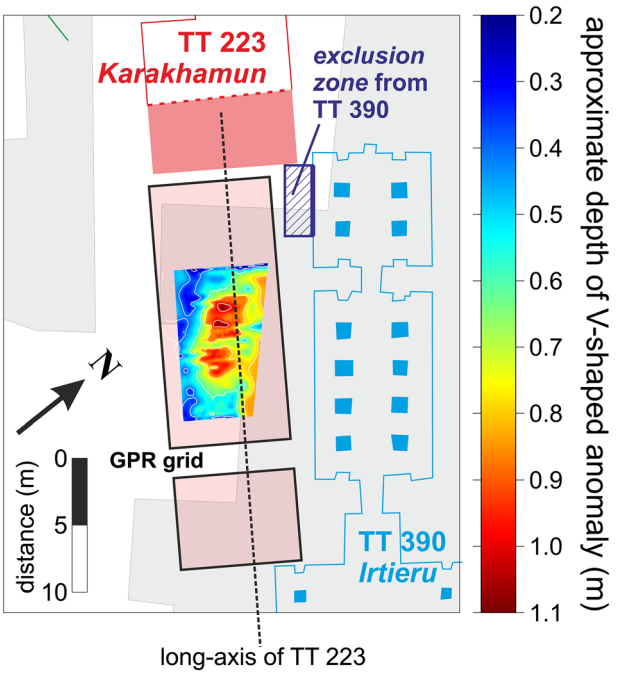

Figure 8. Summary of GPR data, superimposed on the map of the *Karakhamun* tomb. The colour map shows the depth of the 'V-shaped' reflection (white contours at 0.2 m intervals), which extends roughly parallel to the long axis of the tomb. The box extending from the *Irtieru* (TT 390) tomb shows an exclusion zone where, given the lack of reflectivity in the vertically orientated grid 2, there is unlikely to be any continuation of the *Karakhamun* tomb. This figure is available in colour online at wileyonlinelibrary.com/journal/arp

When compared with the likely depth of the tomb superstructure, it is clear that this reflection cannot correspond to either the contact between the limestone and the sediment overburden, or the contact with the air-gap on the underside of any limestone ceiling. Instead, Figure 5b shows very little reflectivity beneath the 'V-shaped' event and, in this sense, the event shows similar characteristics to the reflection from the organic-rich layer observed in the VRP (Figure 4). As such, the V-shaped event is interpreted as a reflection from an organic-rich layer within the sedimentary overburden, and reasons for its geometry are considered in the following section. Of course, the absolute geometry of the events is vulnerable to errors arising from constant velocity migration and depth conversion, but an implausible distribution of velocity variation would be required to attribute this geometry to velocity effects alone. Certain profiles from grid 1 were repeated with 200 MHz antennas in order to investigate improved depth penetration. However, the organic-rich layers also appear to be attenuative to 200 MHz energy (as they did to 500 MHz energy in the VRP survey), and the only reflection that is identifiable in the 200 MHz profiles is a low-resolution image

DOI: 10.1002/arp

of the 'V-shaped' horizon – and no interpretable reflections from the underlying superstructure.

A tentative conclusion from grid 2 is that any continuation of the *Karakhamun* tomb does not pass within 2 m of the *Irtieru* tomb. As such, we define an 'exclusion zone' from the rear chamber of TT 390, within which the continuation of TT 223 cannot be located.

Interpretation of the TT 223 superstructure

Although it is initially disappointing that no direct GPR evidence of the continuation of the *Karakhamun* tomb could be identified, the 'V-shaped' reflection offers indirect support of a structure being present beyond the current edge of excavation. If the 'V-shaped' reflection does arise from within the tomb's sedimentary overburden, it follows that it would have originally been deposited horizontally. In order for this horizon to then adopt the geometry that is apparent in the GPR dataset, some structural deformation must have taken place since its initial deposition and this may be related to the superstructure of the underlying tomb.

Figure 9 shows schematic mechanisms by which an initially horizontal layer could be given a 'V-shaped' geometry. As stated, the initial deposition of the layer will be horizontal (Figure 9a), whether sediment is deposited over a tomb or simply over undisturbed limestone. If the structure of the tomb remains intact, then layering will remain horizontal; however, if there is a subsequent collapse (Figure 9b), it is possible that layering will be deflected downwards as sediments resettle over the disturbed structure. Alternatively, consistent with the analogous *Pabasa* tomb (Figure 2), an open-air staircase could have become progressively filled with sediment; settling of that sediment may then give rise to the downwarped character of the 'V-shaped' reflection (Figure 9c). Clearly, a tomb can only be inferred if there is evidence of either case in Figure 9b or c (an absent tomb has the same 'sedimentary signature' as an intact one), but it follows that if either is evidenced then there should be an underlying structural cause, potentially having archaeological significance.

By the end of the 2011 field campaign some supporting evidence for these interpretations was obtained, as the excavation of TT 223 revealed the lintel of a door in the eastern wall of the courtyard. Focused excavation then provided access to a new vestibule of the *Karakhamun* tomb (Figure 10; Pischikova, 2014b), having dimensions of 2.5 m in width and 7 m in length (length measured parallel to the long axis of the tomb); other than an air-gap of ~1 m height, the vestibule was entirely filled with sediment. At its eastern end, there

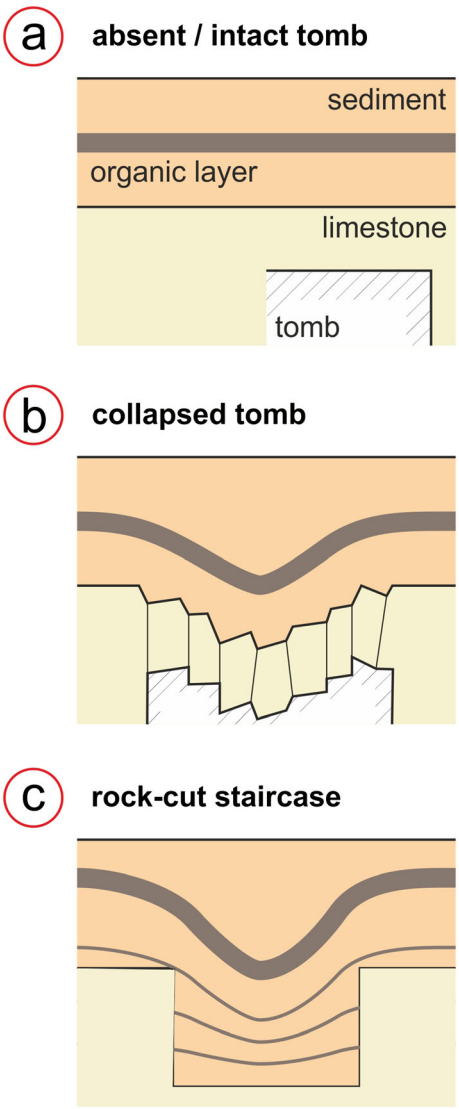

Figure 9. Schematic illustrations to explain the deflection of sedimentary overburden layers, related to tomb structure. (a) Sediment horizons are initially deposited horizontally over intact bedrock, whether that bedrock conceals a tomb or not. (b) A subsequent collapse of the tomb causes downwards deflection of those sedimentary layers. (c) Sediments deposited over an existing cavity, such as the open-air staircase, progressively settle over time and cause downwards deflection of originally horizontal layering. This figure is available in colour online at wileyonlinelibrary.com/journal/arp

was a second lintel implying that the *Karakhamun* tomb almost certainly continues eastwards. Excavations continued at TT 223 during summer 2012, together with more detailed mapping of the tomb layout. These excavations successfully located the onset of the descending staircase, at a position marked in Figure 10 (Pischikova, 2014a). However, the section of staircase between this location and the new vestibule (dashed red line in Figure 10) is yet to be excavated.

DOI: 10.1002/arp

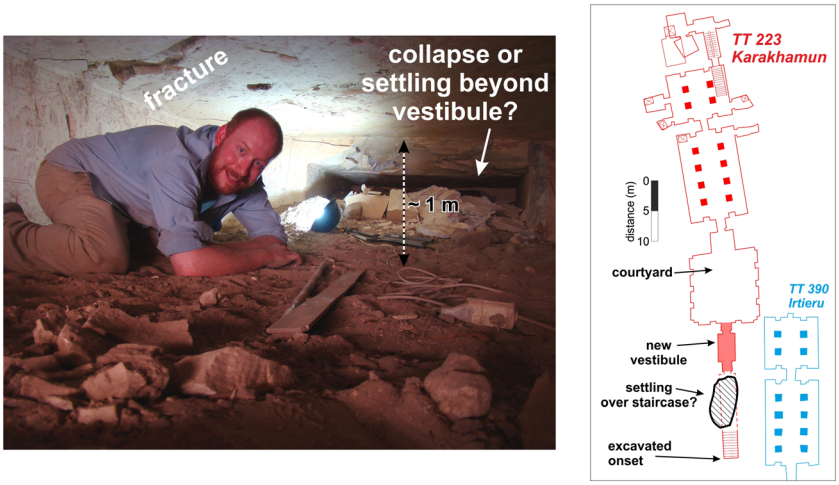

Figure 10. Updated map of the *Karakhamun* tomb, featuring the new vestibule (solid red in map) that was identified in the 2011 field campaign, and the onset of the descending staircase identified in the following year. The GPR surveys show no evidence of deflected overburden horizons immediately above the vestibule, but develop beyond it (~9 m from the courtyard) at a location consistent with the continuation of the staircase (dashed red lines). This figure is available in colour online at wileyonlinelibrary.com/journal/arp

Clearly, there is strong support in these excavation results for the relationships we propose between the 'V-shaped' reflections and the underlying archaeology. We suggested that 'V-shaped' reflections would not be observed over an intact chamber: clearly, the western edge of the intact vestibule in Figure 10 corresponds well with the appearance of the 'V-shaped' reflections. West of the vestibule, the location and orientation of the bowl of the 'V-shaped' reflections correlates well with the likely location of the staircase, hence we attribute the deflection of sediment horizons either to settling over a formerly open-air staircase or the collapse of any roof that covered it. Although excavation would confirm this hypothesis, further geophysical survey would also be useful to this end. The staircase could be a suitable target for characterisation with MASW (multichannel analysis of surface waves; Park *et al.*, 1999) methods. Among the quantities that are obtained from MASW is Poisson's ratio, a measure of the deformation characteristics of a material, and this could usefully distinguish unconsolidated sedimentary infill/overburden from intact and/or fragmented limestone bedrock (e.g. Miller *et al.*, 1999).

Discussion

This paper highlights the potential interpretative benefits of understanding not only the geophysical response of a subsurface target, but also the context of that target within the subsurface and its relationship with the material surrounding and overlying it. Clearly, the optimal scenario for an unambiguous interpretation is to record directly the geophysical response to the subsurface target. However, if the relationship between that target and its host is understood, then the presence of a target can be inferred from diagnostic signatures even if it cannot be imaged itself.

In this paper, the presence of a potentially collapsed tomb superstructure was plausibly inferred from the deflection of sediment horizons in the overburden, which had previously been shown to be highly reflective in initial VRP tests. Although there are a number of mechanisms by which these horizons could have become downwarped, there is nonetheless a compelling match between the location of their maximum deflection and the tomb structure between two sites of excavation. Furthermore, by characterizing GPR propagation through an accessible exposure of host limestone, it became possible to impose a detection criterion on horizons therein. Some local inhomogeneities complicate this simple relationship, but our assumptions were nonetheless validated on revealing the true geometry of the tomb continuation. Therefore, even though our target was buried too deeply to be imaged, an appreciation of potential diagnostic relationships allowed it to be characterized indirectly.

If such diagnostic relationships can be reliably predicted elsewhere, considering for example the geological, geochemical and/or geomorphological relationships between a target and its host material (e.g. Ruffell and McKinley, 2005; Dirix *et al.*, 2013; Weller *et al.*, 2013), then a surveyor has an effective means to extend the capability of a geophysical system even if the target is itself too deep and/or subtle to be imaged. Of course, such inferences are commonplace in the forensic setting, where buried remains do not

DOI: 10.1002/arp

often yield detectable geophysical responses but are located instead from images of disturbances to local soil horizons (Bevan, 1991; Bladon *et al*., 2012). Any number of equivalent scenarios could be envisaged, for example a deep cavity improving the efficiency of near-surface drainage (e.g. Tihansky, 1999) and thereby reducing the electrical conductivity of overlying soils.

Of course, when based on inferential evidence, recommendations for continued study (e.g. further geophysical survey, excavation, etc.) must be made cautiously because uncertainties inherent to the particular geophysical method compound with those associated with the assumed interaction between target and host. However, the consideration of indirect evidence of a subsurface target adds another dimension to the interpretation of a geophysical dataset and may be useful in situations where no direct image of a target can be obtained.

Conclusions

The GPR surveys performed in this paper have allowed a new programme of excavations to be scheduled at the Ancient Egyptian tomb site of South Asasif, Luxor, Egypt. A wider implication of this survey, however, is that archaeological targets can be inferred from geophysical data even if they are not directly imaged themselves. In this way, the effective capabilities of a geophysical system can be extended beyond typical depth limitations. For example, in this survey, our 500 MHz GPR system was able to reveal evidence of a target structure at ~4 m depth even though it is unlikely that the system sampled that structure directly; indeed, 4 m sampling with a 500 MHz wavelet would be considered exceptional in almost any archaeological prospection setting. For such 'inferential' interpretations of geophysical data, an understanding of the relationship between target and host material is required – whether this is established through geophysical methods or other assumed and/or measured relationships. We suggest that, even if a prospective target is deemed to be beyond the capabilities of a geophysical survey system itself, indirect methods can be usefully applied to predict its presence in the ground.

Acknowledgements

The fieldwork in Egypt was supported by a Swansea University 'Bridging the Gaps' grant, and GPR antennas were provided by the NERC Geophysical Equipment Facility (Loan 951). Tavi Murray assisted with the funding application for this work. The Egyptian Supreme Council for Antiquities granted access to the South Asasif tombs. Adam Booth was supported at the time of survey by the Swansea University GLIMPSE project. ReflexW© processing software was provided to Imperial College London with support from The Hajar Project. The manuscript was improved with useful comments from two anonymous reviewers and Dr Lawrence Conyers in his editorial role.

References

Annan AP. 2005. Ground penetrating radar. In Near Surface Geophysics, Butler D (ed.). Society of Exploration Geophysicists: Tulsa, OK; 357–438.

Bevan B. 1991. The search for graves. *Geophysics* **56**: 1310–1319.

Bladon P, Moffat I, Guilfolye D, Beale A, Milani J. 2012. Mapping anthropogenic fill with GPR for unmarked grave detection: a case study from a possible location of Mokare's grave, Albany, Western Australia. *Exploration Geophysics* **42**(4): 249–257.

Booth AD, Linford NT, Clark RA, Murray T. 2008. Three-dimensional, multi-offset ground penetrating radar imaging of archaeological targets. *Archaeological Prospection* **15**(2): 93–112.

Buursink ML, Lane JW, Clement WP, Knoll MD. 2002. Use of vertical radar profiling to estimate porosity at two New England sites and comparison with neutron porosity log. *Symposium on the Application of Geophysics to Engineering and Environmental Problems*, Las Vegas, Nevada.

Conyers LB. 2013. Ground-Penetrating Radar for Archaeology, 3rd edn. AltaMira Press: Walnut Creek, CA.

Creasman PP, Sassen D. 2011. Remote sensing. In The Temple of Tausret: The University of Arizona Egyptian Expedition Tausret Temple Project, 2004–2011. University of Arizona Egyptian Expedition: USA, 150–159.

Dirix K, Muchez P, Degryse P, Kaptijn E, Mušič B, Vassilieva E, Poblome J. 2013. Multi-element soil prospection aiding geophysical and archaeological survey on an archaeological site in suburban Sagalassos (SW-Turkey). *Journal of Archaeological Science* **40**(7): 2961–2970.

Eigner D. 1984. *Die monumentalen Grabbauten der Spätzeit in der Thebanischen Nekropole*, Plan 9. Verlag der Österreichen Akademie der Wissenschaften: Vienna.

Featherstone R, Horne P, Macleod D, Bewley R. 1999. Aerial reconnaissance over England in summer 1996. *Archaeological Prospection* **6**(2): 47–62.

Grasmueck M, Weger R, Horstmeyer H. 2005. Full resolution GPR imaging. *Geophysics* **70**: K1–K19.

Jol HM, Bauman P, Bahat D. 2006. Looking into the Western Wall, Jerusalem, Israel. *Proceedings of the 11th International Conference on Ground Penetrating Radar*, Columbus, OH, June 19–22.

Li N. 2012. Trace interpolation investigation for anti-aliasing and 2-D migration image improvement. Unpublished MSc Thesis, MSc Petroleum Geophysics, Imperial College London.

Miller RD, Xia J, Park CB, Ivanov J, Williams E. 1999. Using MASW to map bedrock in Olathe, Kansas. *SEG Technical Program Expanded Abstracts* 433–436. DOI: 10.1190/1.1821045.

Park CB, Miller RD, Xia J. 1999. Multichannel analysis of surface waves. *Geophysics* **64**(3): 800–808.
Pischikova E. 2008. Tomb of Karakhamun (TT 223) in the South Asasif and a 'Lost' Capital. *Journal of the American Research Center in Egypt* **44**: 185–192.
Pischikova E. 2009. The early Kushite Tombs of South Asasif. *British Museum Studies in Ancient Egypt and Sudan* **12**: 11–30.
Pischikova E. 2014a. Kushite tombs of the South Asasif Necropolis: conservation, reconstruction and research. In Thebes in the First Millennium BC, Pischikova E, Budka J, Griffin K (eds). Cambridge Scholars Publishing: Newcastle upon Tyne, UK.
Pischikova E. 2014b. Tombs of the South Asasif Necropolis: Thebes, Karakhamun (TT223), and Karabasken (TT 391) in the Twenty-Fifth Dynasty, English edn. The American University in Cairo Press: Cairo.
Ruffell A, McKinley J. 2005. Forensic geoscience: applications of geology, geomorphology and geophysics to criminal investigations. *Earth-Science Reviews* **69**(3–4): 235–247.
Tihansky AB. 1999. Sinkholes, Western Florida. In Land Subsidence in the United States, Galloway D, Jones DR, Ingebritsen SE (eds). Circular 1182, US Geological Survey: Reston, Virginia; 121–140.
Vignoli G, Deiana R, Cassiani G. 2012. Focused inversion of vertical radar profile (VRP) traveltime data. *Geophysics* **77**(1): H9–H18.
Weaver W. 2006. GPR mapping in clay: success from South Carolina, USA. *Archaeological Prospection* **13**: 147–150.
Welc F, Trzcínski J, Kowalczyk S, Mieszkowski R. 2013. Geophysical survey (GPR) in West Saqqara (Egypt): Preliminary remarks. *Studia Quaternia* **30**(2): 99–108.
Weller A, Rosas S, Eidner E, Hartsch K. 2013. Geophysical, petrographic and geochemical survey on the Nazca Lines. *Journal of Earth Science and Engineering* **3**: 159–167.
Witten AJ, Levy TE, Adams RB, Won IJ. 2000. Geophysical surveys in the Jebel Hamrat Fidan, Jordan. *Geoarchaeology* **15**(2): 135–150.

DOI: 10.1002/arp